COBEM 2021 26th International Congress of Mechanical Engineering
November 22-26, 2021, Virtual Congress, Brazil

COB-2021-1309
Steam generator efficiency simulation with a multi-fidelity approach

Augusto Delavald Marques
Lara Werncke Vieira
Jéssica Duarte
Julian Hunt
Paulo Smith Schneider
Federal University of Rio Grande do Sul
augusto.marques@ufrgs.br
lara.vieira@ufrgs.br
jessica.jd.duarte@gmail.com
hunt@iiasa.ac.at
pss@mecanica.ufrgs.br

Abstract. *This paper presents the simulation of a real steam generator from a coal-fired power plant with a multi-fidelity model. The model's purpose is to calculate the steam generator efficiency in different operating situations. The proposed approach combines data from an energy balance-based model, the low fidelity approach, and data from actual measurements, the high fidelity information. Fifty-four simulations with the commercial software Ebsilon composes the low fidelity dataset to be completed with seven experiments conducted in a real power plant. The two datasets are used to build a multi-fidelity model with the Co-kriging methodology, which combines the predicted system behavior by the low fidelity model with the accurate results from the high-fidelity dataset. The four cases assessed in this paper show that the maximum absolute error for the system efficiency dropped from* 0.57% *for the low fidelity model to* 0.18% *with the multi-fidelity approach.*

Keywords: *Multi-fidelity model, Co-kriging, Gaussian process, Steam generator model*

1. INTRODUCTION

Steam generators are complex equipment used to convert chemical energy from fuel to heat energy and uses this energy to convert water into steam. There has been an increasing demand to operate the thermal power plant boilers in a more flexible and agile manner due to renewable energy penetration, excess generation capacity, online trading, etc.(Sunil *et al.*, 2017). Several works have performed physics-based modeling of this equipment. Bhambare *et al.* (2007) proposed the division of the steam generator into 7 subcomponents and performed modeling using the SIMULINK® software aiming the steam generator control, the authors validated the model with data from a 250 MW plant and obtained errors around 5 bar in the main steam pressure. Lee (2003) developed and compared two models for predicting the main steam conditions at the steam generator outlet, a parametric model and a model based on neural networks. Both models were shown to be able to predict the flow rate based on steam generator parameters, showing a maximum error of 8.66%. Said *et al.* (2011) modeled the furnace of a steam generator in different operating situations, his simulation shows a temperature of 1600 K near the furnace outlet. Hajebzadeh *et al.* (2019) simulated a steam generator with tangential firing with gas recirculation. In the model validation, he obtained a maximum error of 7.3 % in the flue gas temperature. Grądziel (2019) modeled the mass flow rate and heat transfer of the natural circulation occurring between the flue and water walls of a steam generator, obtained errors of 5.7% in the calculated flow rate relative to a measured point. Pure physics models are complex to build and can require high computing power. Even then, they may not be able to cover all the physics of the problem, either due to simplifications of the model or due to a lack of system information. More recently papers propose data-driven models for the steam generator (Dhanuskodi *et al.* (2015), Hu *et al.* (2020)).

This paper is a sequence of two previous works (Vieira (2020) and Vieira *et al.* (2020)) and aims to build a multi-fidelity model based on the Co-Kriging method (Forrester *et al.*, 2007) to a coal-fired boiler single-furnace unit, which supplies a 360 MW power plant situated in the port of PECÉM, Brazil.

2. METHODOLOGY

Figure 1 shows the methodology adopted to construct and assess a steam generator multi-fidelity model.

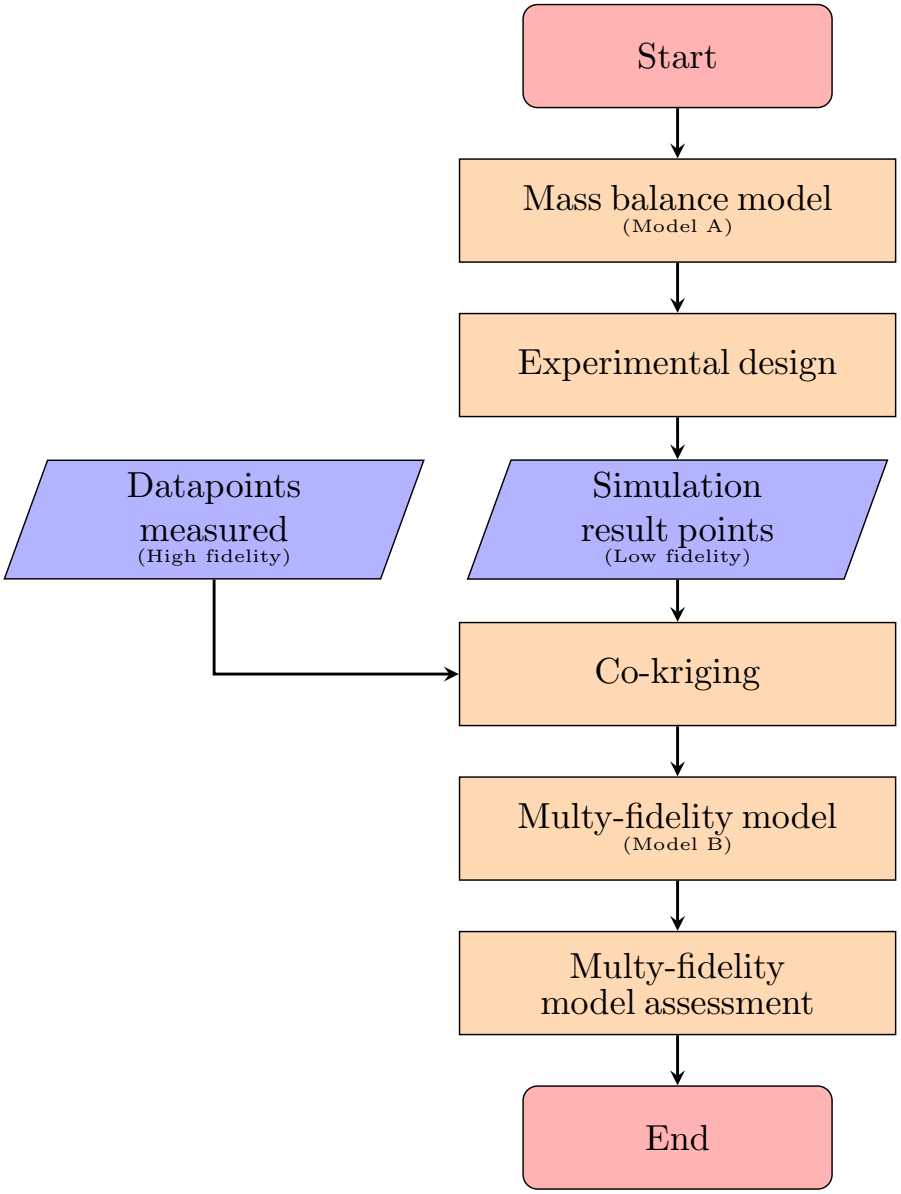

Figure 1: Methodology adopted to construct and assess a steam generator multi-fidelity model.

A mass balance model of the steam generator is built, hereafter referred to as Model A. The objective of this model is to generate results data points, these data points are viewed as low fidelity data when in regards to the data measured. An experimental design is a specification of points (runs) in the experimental region at which the response is to be computed (Santner *et al.*, 2003). The Box–Behnken design (Box and Behnken, 1960) generates a design matrix used to conduct the simulations on Model A. The simulation results are used as low fidelity data with the high fidelity data to feed the Co-kriging algorithm. The measured points used as high fidelity data are from the PECÉM Power Plant. The Co-kriging method produces a multi-fidelity model, hereafter referred to as Model B.

2.1 Mass balance simulation

Figure 2 shows the representation of the steam generator in the Ebsilon® simulation program. In this software, it is simulated all main steam generator components, from the mills to the working fluid and flue gas paths that goes through the equipment.

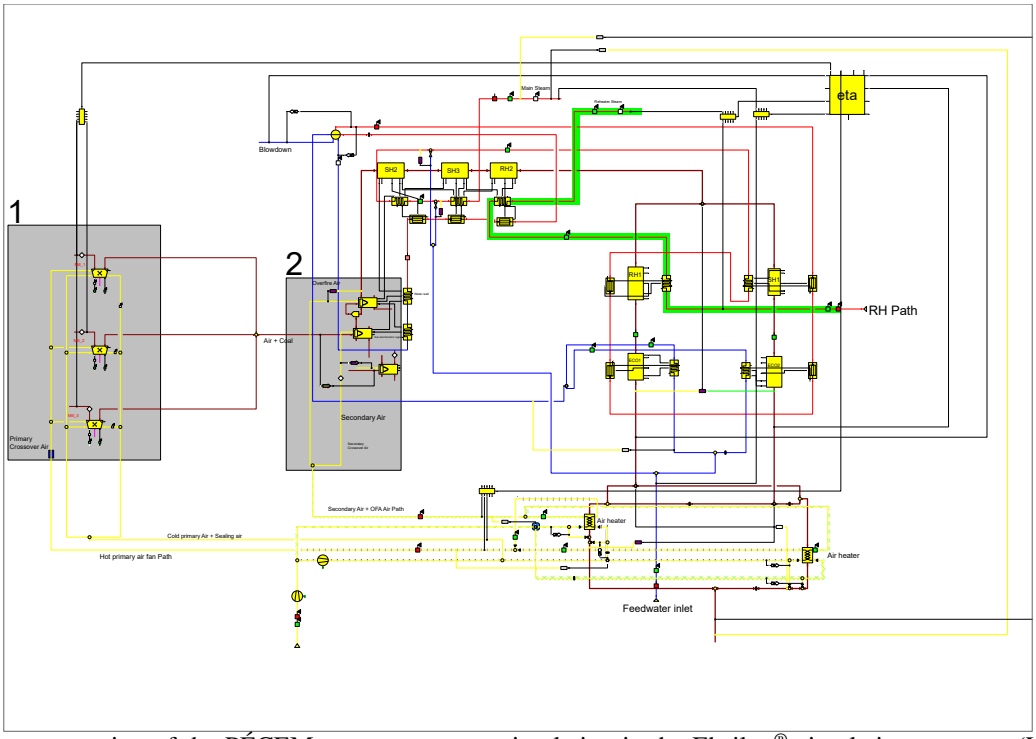

Figure 2: Representation of the PÉCEM steam generator simulation in the Ebsilon® simulation program (Vieira *et al.*, 2020).

The model of the steam generator consists of 149 components, the input parameters in the simulations are located in the region of the mills (1) and in the region of the furnace (2).

The Ebsilon® mill component has as input the hot and cold primary air, the coal flow, and sealing air. It also allows setting the temperature of the mixture between the hot and cold primary air, and the outlet temperature of the coal and air mixture. It is also possible to see in region 1 the crossover region. The three outlets of the mills are mixed and directed to the furnace, located in region 2. In region 2, two components are used to represent the sub-stoichiometric part and the excess air part of the furnace. In this region, secondary airflow is imposed directly and, also Overfire Air is imposed through the percentage of O_2 present in the combustion gases. Its output is the flue gases sends to the heat exchangers and the working fluid in a biphasic state, directed to the pipe. Although the model only performs simulations in steady-state, it has operating curves for the components and, therefore allows simulating different operating conditions as off-design from a defined design situation.

The only parameter that is not possible to integrate into the model is the mill classifier speed (P3), thus this parameter is not included in any analysis. The result of interest in this simulation is the steam generator efficiency calculated by the direct method (Shah and Adhyaru, 2011).

2.2 Box–Behnken design

Box-Behnken designs (BBD) are a class of rotatable or nearly rotatable second-order designs based on three-level incomplete factorial designs. The number of experiments (N) required for the development of BBD is defined according to Equation 1 (Ferreira *et al.*, 2007).

$$N = 2k(k-1) + C_O \tag{1}$$

where k is number of factors and C_O is the number of central points. Table 1 presents the design matrix construct with the Box–Behnken design.

The design matrix construct by a Box–Behnken design with the seven parameters results in 54 experiments performed in Model A.

Table 1: Design matrix for the Model A simulations. Adapted from Vieira *et al.* (2020)

Experiment	P1	P2	P4	P5	P6	P7	Experiment	P1	P2	P4	P5	P6	P7
1	28	75	0,800	2,25	1020,5	1085,0	28	26	75	0,875	2,25	1020,5	1077,5
2	28	85	0,875	3,00	1020,5	1077,5	29	26	65	0,800	2,25	1018,0	1077,5
3	28	65	0,875	3,00	1020,5	1077,5	30	26	75	0,875	2,25	1020,5	1077,5
4	28	65	0,875	1,50	1020,5	1077,5	31	26	85	0,875	2,25	1018,0	1070,0
5	26	75	0,875	2,25	1020,5	1077,5	32	26	85	0,875	2,25	1018,0	1085,0
6	26	85	0,875	2,25	1023,0	1085,0	33	24	65	0,875	1,50	1020,5	1077,5
7	26	75	0,800	1,50	1020,5	1085,0	34	28	75	0,875	1,50	1023,0	1077,5
8	26	85	0,800	2,25	1023,0	1077,5	35	24	65	0,875	3,00	1020,5	1077,5
9	26	75	0,950	1,50	1020,5	1085,0	36	24	75	0,800	2,25	1020,5	1085,0
10	26	65	0,950	2,25	1018,0	1077,5	37	26	65	0,875	2,25	1018,0	1070,0
11	28	75	0,875	3,00	1018,0	1077,5	38	26	85	0,875	2,25	1023,0	1070,0
12	24	75	0,800	2,25	1020,5	1070,0	39	26	65	0,875	2,25	1023,0	1070,0
13	26	65	0,875	2,25	1023,0	1085,0	40	26	75	0,800	3,00	1020,5	1070,0
14	28	75	0,950	2,25	1020,5	1085,0	41	26	65	0,950	2,25	1023,0	1077,5
15	24	75	0,950	2,25	1020,5	1070,0	42	26	65	0,875	2,25	1018,0	1085,0
16	26	85	0,800	2,25	1018,0	1077,5	43	28	75	0,875	1,50	1018,0	1077,5
17	26	75	0,950	3,00	1020,5	1085,0	44	26	75	0,875	2,25	1020,5	1077,5
18	26	75	0,950	1,50	1020,5	1070,0	45	26	65	0,800	2,25	1023,0	1077,5
19	28	75	0,950	2,25	1020,5	1070,0	46	28	75	0,875	3,00	1023,0	1077,5
20	26	75	0,875	2,25	1020,5	1077,5	47	24	75	0,875	1,50	1023,0	1077,5
21	24	75	0,875	1,50	1018,0	1077,5	48	28	75	0,800	2,25	1020,5	1070,0
22	24	75	0,875	3,00	1018,0	1077,5	49	28	85	0,875	1,50	1020,5	1077,5
23	24	85	0,875	1,50	1020,5	1077,5	50	26	75	0,800	1,50	1020,5	1070,0
24	26	75	0,800	3,00	1020,5	1085,0	51	26	85	0,950	2,25	1023,0	1077,5
25	24	75	0,875	3,00	1023,0	1077,5	52	26	75	0,875	2,25	1020,5	1077,5
26	26	85	0,950	2,25	1018,0	1077,5	53	24	75	0,950	2,25	1020,5	1085,0
27	24	85	0,875	3,00	1020,5	1077,5	54	26	75	0,950	3,00	1020,5	1070,0

2.3 Datapoints

Table 2 shows the points of the experiments performed by Vieira (2020) at PECEM Power Plant.

Table 2: Datapoints from experment conducted ad PECEM power plant (Vieira, 2020).

Experiment	P1 (kg/s)	P2 (°C)	P3 (rpm)	P4 (%)	P5 (%)	P6 (mbar)	P7 (mbar)	Efficiency (%)
1	26.0	65	90	0.88	2.3	23	78	84.19
2	24.0	75	100	0.88	2.3	18	70	84.37
3	26.0	75	100	0.80	3.0	23	78	84.02
4	26.0	75	100	0.80	3.0	18	78	82.89
5	26.0	75	100	0.88	2.3	21	78	83.90
6	24.0	75	110	0.88	3.0	21	78	83.61
7	26.0	65	100	0.88	3.0	21	85	83.19
8	28.0	75	100	0.88	2.3	23	85	83.76
9	26.0	85	100	0.88	3.0	21	85	82.92
10	24.0	75	100	0.88	2.3	18	85	82.82
11	24.0	85	100	0.95	2.3	21	78	83.71

This information is used as high fidelity data points since they are real measures of the system of interests. The P1-P7 parameters stand for primary air mass flow rate, pulverized coal outlet, the speed of the dynamic classifier, O_2 excess, secondary air pressure and, primary air pressure, respectively.

Figure 3 presents the results of these simulations and the efficiency points from the experiments 1 up to 7 from Tab. 2.

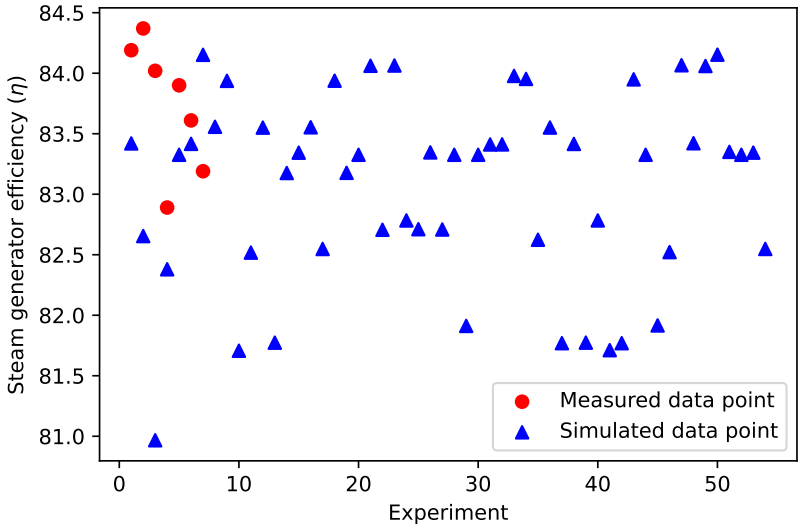

Figure 3: Simulated data points and measured values.

The red dots comprises the $Y_e(X_e)$ from Eq. 3 and the blue triangles comprise the set $Y_c(X_c)$, among which 54 correspond to results considered of low fidelity and 7 points considered of high fidelity.

2.4 Co-kriging and Multy-fidelity model

Equation (2) up to Eq. (9) follows the Forrester *et al.* (2007) paper. There are two sets of entries, X_e associated with an unknown or expensive function to evaluate, and another set X_c associated with a known and easy to evaluate function. Equation (2) shows the concatenation of these two sets,

$$X = \begin{bmatrix} X_c \\ X_e \end{bmatrix} = [\boldsymbol{x}_c^{(1)}, .., \boldsymbol{x}_c^{(n_c)}, \boldsymbol{x}_e^{(1)}, .., \boldsymbol{x}_e^{(n_e)}]^T \tag{2}$$

the two sets can be of different sample sizes, n_c and n_e. The subscript c stands for *cheap* and e for *expensive*.

Equation (3) shows the concatenation of the known responses of the two functions, the expensive function to be evaluated $Y_e(X_e)$ the cheap function $Y_c(X_c)$.

$$Y = \begin{bmatrix} Y_c(X_c) \\ Y_e(X_e) \end{bmatrix} = [Y_c(\boldsymbol{x}_c^{(1)}), .., Y_c(\boldsymbol{x}_c^{(n_c)}), Y_e(\boldsymbol{x}_e^{(1)}), .., Y_e(\boldsymbol{x}_e^{(n_e)})]^T \tag{3}$$

It is assumed that the data for both fidelities can be modeled as $\mathcal{GP}$ gaussian processes. Equation (4) presents the form of association between the processes.

$$\mathcal{GP}_e(\boldsymbol{x}) = \rho \mathcal{GP}_c(\boldsymbol{x}) + \mathcal{GP}_d(\boldsymbol{x}) \tag{4}$$

It is stated that it is possible to estimate the expensive process $\mathcal{GP}_e(\boldsymbol{x})$ by a cheap process $\mathcal{GP}_c(\boldsymbol{x})$ multiplied by a scaling factor ρ plus a Gaussian process $\mathcal{GP}_d(\boldsymbol{x})$ that represents the difference between $\mathcal{GP}_e(\boldsymbol{x})$ and $\mathcal{GP}_c(\boldsymbol{x})$.

Equation (5) presents the prediction of the expensive function given by the multi-fidelity model.

$$\hat{y}_e(\boldsymbol{x}^{(n_e+1)}) = \hat{\boldsymbol{\mu}} + \boldsymbol{c}^T \boldsymbol{C}^{-1}(\boldsymbol{y} - \mathbf{1}\hat{\boldsymbol{\mu}}) \tag{5}$$

where the predicted mean is given by Eq. (6).

$$\hat{\boldsymbol{\mu}} = \mathbf{1}^T \boldsymbol{C}^{-1} \boldsymbol{y} / \mathbf{1}^T \boldsymbol{C}^{-1} \mathbf{1} \tag{6}$$

The complete covariance matrix is given by Eq. 7.

$$\boldsymbol{C} = \begin{bmatrix} \sigma_c^2 \boldsymbol{\Psi}_c(\boldsymbol{X}_c, \boldsymbol{X}_c) & \rho\sigma_c^2 \boldsymbol{\Psi}_c(\boldsymbol{X}_c, \boldsymbol{X}_e) \\ \rho\sigma_c^2 \boldsymbol{\Psi}_c(\boldsymbol{X}_e, \boldsymbol{X}_e) & \rho^2\sigma_c^2 \boldsymbol{\Psi}_c(\boldsymbol{X}_e, \boldsymbol{X}_e) + \sigma_d^2 \boldsymbol{\Psi}_d(\boldsymbol{X}_e, \boldsymbol{X}_e) \end{bmatrix} \tag{7}$$

where σ^2 is de variance and $\boldsymbol{c}$ is defined as a column vector of the covariance $\boldsymbol{X}$ and $\boldsymbol{x^{(n_e+1)}}$

$$\boldsymbol{c} = \begin{bmatrix} \hat{\rho}\hat{\sigma}_c^2 \boldsymbol{\Psi}_c(\boldsymbol{X}_c, x^{(n+1)}) \\ \hat{\rho}^2\hat{\sigma}_c^2 \boldsymbol{\Psi}_c(\boldsymbol{X}_e, x^{(n+1)}) + \hat{\sigma}_d^2 \boldsymbol{\Psi}_d\left(\boldsymbol{X}_e, x^{(n+1)}\right) \end{bmatrix} \tag{8}$$

One correlation of the matrix of correlations $\boldsymbol{\Psi}$ is expressed by Eq. (9).

$$\psi^{(i)} = \exp\left(-\sum_{j=1}^{k} \hat{\theta}_j ||x_j^{(n+1)} - x_j^{(i)}||^{\hat{p}_j}\right) \tag{9}$$

As we can notice $\psi = 1$ when the distance goes to zero and $\psi = 0$ when the distance tends to infinity. The θ_j and p_j are hyper-parameters to estimate.

3. RESULTS

Figure 4 presents the results obtained with the multi-fidelity model for the four points of the test set.

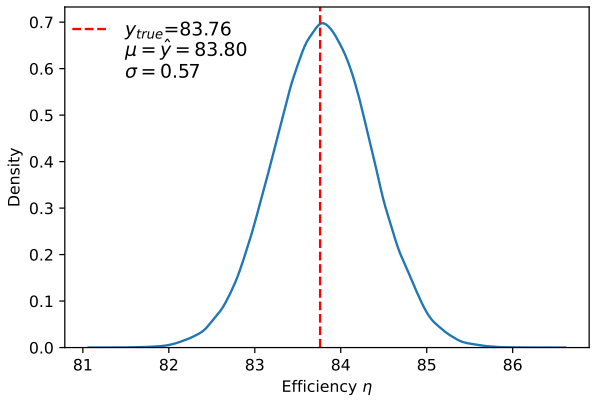

(a) Multi-fidelity result and the true efficiency for the 8th experiment.

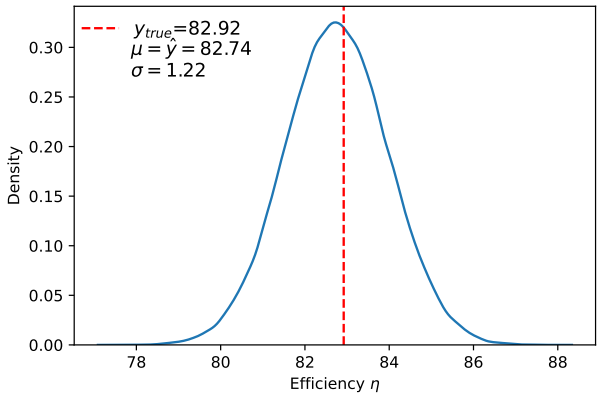

(b) Multi-fidelity result and the true efficiency for the 9th experiment.

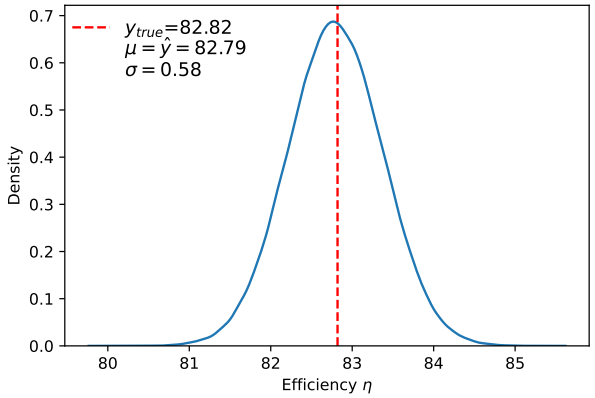

(c) Multi-fidelity result and the true efficiency for the 10th experiment.

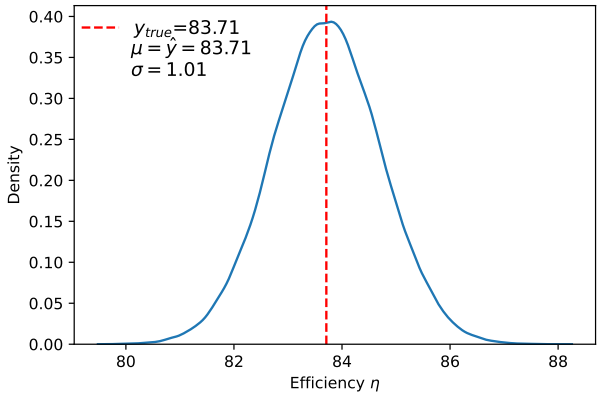

(d) Multi-fidelity result and the true efficiency for the 11th experiment.

Figure 4: Comparison of the efficiency results obtained with the multi-fidelity model and the test subset true values.

Figure 5 presents the efficiency values for experiments 8th through 11th in Table 2. The values of P1 through P7 (except P3) of the respective rows were used as input data for the energy and mass balance model and the multi-fidelity model.

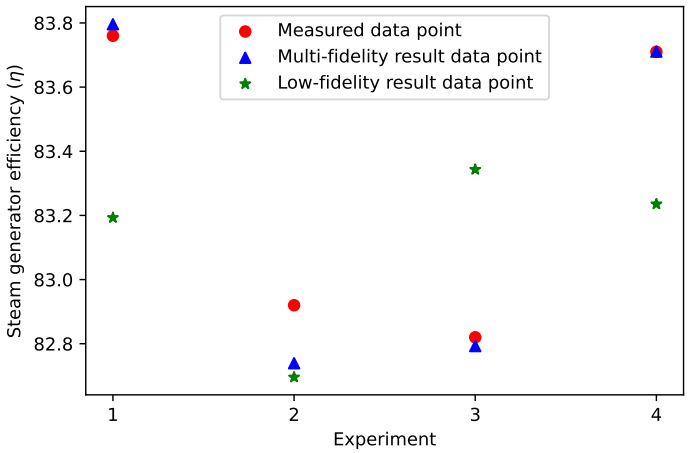

Figure 5: Comparison of the test subset efficiency values with the values obtained from the mass and energy balance simulation and the multi-fidelity model.

Although Model A was able to obtain results similar to the actual values, the multi-fidelity model could obtain a better result in the four cases tested. It is noteworthy that in addition to the 54 points of Model A, for testing purposes, only seven points considered to have high fidelity were used as building information for Model B. If all available high-fidelity points were used, better result are expected. The maximum absolute error of the efficiency value was 0.57 % for Model A and 0.18 % for Model B. Note that the predicted mean value is close to the actual value in all four cases, being, in all cases, less than one standard deviation from the mean.

4. CONCLUSIONS

The steam generator studied is from a thermal power plant in Brazil, and its understanding is essential to have a more flexible operation.

The Co-kriging method was applied to build a steam generator multi-fidelity model. From a balance-based model, 54 simulations were used to generate steam generator efficiency points. The data of 7 experiments were used as high fidelity information for training the multi-fidelity model. Another 4 experiments available were kept out of training and used to verify the new model. The multi-fidelity was capable of better representing the equipment than the original only balance-based model. The method coupled the available information with the purely physics-based model to build a new function better represents the steam generator. Further improvements may explore different parameter combinations and the quantity of low and high-fidelity information needed.

5. ACKNOWLEDGEMENTS

We acknowledge Energy of Portugal EDP for technical support to this project; A.D.Marques acknowledges the financial support from CNPq 132422/2020-4 for his MSc grant;L.W.Vieira acknowledges the financial support from CAPES 88882.346360/2014-01 for her Ph.D. grant; J.Duarte acknowledges the financial support from CNPq 154147/2020-6 for her undergraduate scholarship; P.S. Schneider acknowledges CNPq for his research grant (PQ 305357/2013-1).

6. REFERENCES

Bhambare, K., Mitra, S.K. and Gaitonde, U., 2007. "Modeling of a coal-fired natural circulation boiler". *Journal of Energy Resources Technology*, Vol. 129, No. 2, pp. 159–167.

Box, G.E. and Behnken, D.W., 1960. "Some new three level designs for the study of quantitative variables". *Technometrics*, Vol. 2, No. 4, pp. 455–475.

Dhanuskodi, R., Kaliappan, R., Suresh, S., Anantharaman, N., Arunagiri, A. and Krishnaiah, J., 2015. "Artificial neural networks model for predicting wall temperature of supercritical boilers". *Applied Thermal Engineering*, Vol. 90, pp. 749–753.

Ferreira, S.C., Bruns, R., Ferreira, H., Matos, G., David, J., Brandão, G., da Silva, E.P., Portugal, L., Dos Reis, P., Souza, A. *et al.*, 2007. "Box-behnken design: an alternative for the optimization of analytical methods". *Analytica chimica acta*, Vol. 597, No. 2, pp. 179–186.

Forrester, A.I., Sóbester, A. and Keane, A.J., 2007. "Multi-fidelity optimization via surrogate modelling". *Proceedings of the royal society a: mathematical, physical and engineering sciences*, Vol. 463, No. 2088, pp. 3251–3269.

Grądziel, S., 2019. "Analysis of thermal and flow phenomena in natural circulation boiler evaporator". *Energy*, Vol. 172, pp. 881–891.

Hajebzadeh, H., Ansari, A.N. and Niazi, S., 2019. "Mathematical modeling and validation of a 320 mw tangentially fired boiler: A case study". *Applied Thermal Engineering*, Vol. 146, pp. 232–242.

Hu, X., Niu, P., Wang, J. and Zhang, X., 2020. "Multi-objective prediction of coal-fired boiler with a deep hybrid neural networks". *Atmospheric Pollution Research*, Vol. 11, No. 7, pp. 1084–1090.

Lee, Won Uk e Yeo, Y.K., 2003. "Steady-state modeling of coal boilers". *Korean Journal of Chemical Engineering*, Vol. 20, No. 3, pp. 436–439.

Said, S.A.M., Habib, M.A., Badr, H.M., Ben-Mansour, R. and Al-Anizi, S., 2011. "Analysis of water circulation in boilers under steady-state conditions". *Computational Thermal Sciences: An International Journal*, Vol. 3, No. 4.

Santner, T.J., Williams, B.J., Notz, W.I. and Williams, B.J., 2003. *The design and analysis of computer experiments*, Vol. 1. Springer.

Shah, S. and Adhyaru, D., 2011. "Boiler efficiency analysis using direct method". In *2011 Nirma University International Conference on Engineering*. IEEE, pp. 1–5.

Sunil, P., Barve, J. and Nataraj, P., 2017. "Mathematical modeling, simulation and validation of a boiler drum: Some investigations". *Energy*, Vol. 126, pp. 312–325.

Vieira, L.W., 2020. "Standardization of steam generator operation in order to increase performamce through process surrogate models".

Vieira, L.W., Marques, A.D., Duarte, J., Zanardo, R.P., Schneider, P.S., Siluk, J.C.M. and Oliveira, G.L.B.d., 2020. "Surrogate modeling approach to standardize a steam generator operation: a case study of the pecem power plant". In *Iberian Latin-American Congress on Computational Methods in Engineering (41.: 2020: On-line). Proceedings [recurso eletrônico]. São Paulo: ABMEC, 2020.*

7. RESPONSIBILITY NOTICE

The authors are solely responsible for the printed material included in this paper.